

Detection of spin and charge states in centrosymmetric materials by nonlinear optics

Takuya Satoh^{a)}

Max-Born-Institut, Max-Born-Straße 2A, 12489 Berlin, Germany and Research Center for Advanced Science and Technology, The University of Tokyo, Tokyo 153-8904, Japan

Thomas Lottermoser and Manfred Fiebig

Max-Born-Institut, Max-Born-Straße 2A, 12489 Berlin, Germany

Yasushi Ogimoto, Hiroharu Tamaru, Makoto Izumi, and Kenjiro Miyano

Research Center for Advanced Science and Technology, The University of Tokyo, Tokyo 153-8904, Japan

(Presented on 8 November 2004; published online 2 May 2005)

Nonlinear optics is applied to two types of centrosymmetric magnetic materials and shown to be a powerful complement to linear optics. (i) For the investigation of centrosymmetric bulk compounds resonance-enhanced sum-frequency generation is introduced and found to be particularly useful for the investigation of antiferromagnets. The technique is demonstrated on antiferromagnetic NiO. (ii) The interfaces of centrosymmetric thin films are investigated on manganite heterostructures by interface-sensitive second-harmonic generation. Maker fringes reveal a valence difference of Mn ions at the heterointerface. Comparison with a model calculation shows good agreement. © 2005 American Institute of Physics. [DOI: 10.1063/1.1851676]

I. INTRODUCTION

Nonlinear optics is a powerful complement to linear optics because of the additional degrees of freedom arising from the involvement of two or more different light fields.¹ Since the second-order optical susceptibility $\chi^{(2)}$ depends on site symmetry, the nonlinear optical response may change drastically by a subtle modulation of symmetry even if it cannot be detected by alternative techniques probing the macroscopic physical properties. The most common nonlinear optical process is second-harmonic generation (SHG). Recently SHG has been introduced for the investigation of magnetic materials.^{2,3} In particular, SHG is useful for the investigation of antiferromagnetic systems where linear magneto-optical effects such as Faraday and Kerr rotations are too small or not applicable at all because of the absence of a macroscopic magnetization.

Unfortunately, SHG in leading-order [electric dipole (ED)] approximation of the light field is only allowed in noncentrosymmetric systems¹ which constitute the minority of magnetic materials. In order to solve this problem, two approaches are described in the present work. If the magnetic bulk properties are of interest, higher-order nonlinear effects such as magnetic-dipole (MD) -type SHG (Refs. 4 and 5) and third-order nonlinear optical processes can be employed.⁶ If, on the other hand, magnetic surface or interface properties are of interest, ED-type SHG is a unique probe because the inversion symmetry is broken at the boundary of the material.²

In Sec. II, resonance-enhanced magnetic sum-frequency generation (SFG) is introduced as a tool for the investigation of magnetically ordered bulk compounds. Magnetic SFG is

employed to fix the photon energy $\hbar\omega_1$ of one incident light field at the energy of an intermediate electronic transition while the photon energy $\hbar\omega_2$ of the other incident light field is tuned in order to scan the nonlinear spectrum at $\hbar(\omega_1 + \omega_2)$. Even if the transition to the intermediate state at $\hbar\omega_1$ is only weakly allowed, as is the case for a MD transition, the small transition rate is compensated by resonance enhancement at $\hbar\omega_1$ which amplifies the nonlinear signal by orders of magnitude. The technique is demonstrated on NiO, a centrosymmetric antiferromagnet of great current interest due to its high Néel temperature $T_N=523$ K.

In Sec. III, interface-sensitive SHG is applied to a manganite thin-film heterostructure. The interface of the transition-metal oxides is an attractive topic for fundamental physics and application. Since the electronic state is sensitive to carrier doping level and lattice constant in the strongly correlated transition-metal oxides, an appearance of new phases, spin canting, and spin frustration due to charge transfer, as well as strain effects and exchange interaction at the interface have been proposed.^{7,8} For application, the dead layer at the interface suppresses the tunneling magnetoresistance in manganite thin film near the Curie temperature.⁹ Thus, it is necessary to clarify the spin and charge states of the interface. We fabricated four manganite thin films (LaMnO_3 , SrMnO_3 , $\text{SrMnO}_3/\text{LaMnO}_3$, and $\text{LaMnO}_3/\text{SrMnO}_3$) in which the valence of Mn ion is 3+ for LaMnO_3 while 4+ for SrMnO_3 . ED-type SHG is observed due to the valence difference of Mn ions at the interface.

II. RESONANCE-ENHANCED MAGNETIC SFG

Since in centrosymmetric materials, ED-type SFG is forbidden,¹ the second-order nonlinear polarization $\mathbf{P}(\omega_1 + \omega_2)$ in NiO in the case of two-photon SFG is expressed by

^{a)}Electronic mail: satoh@mbi-berlin.de

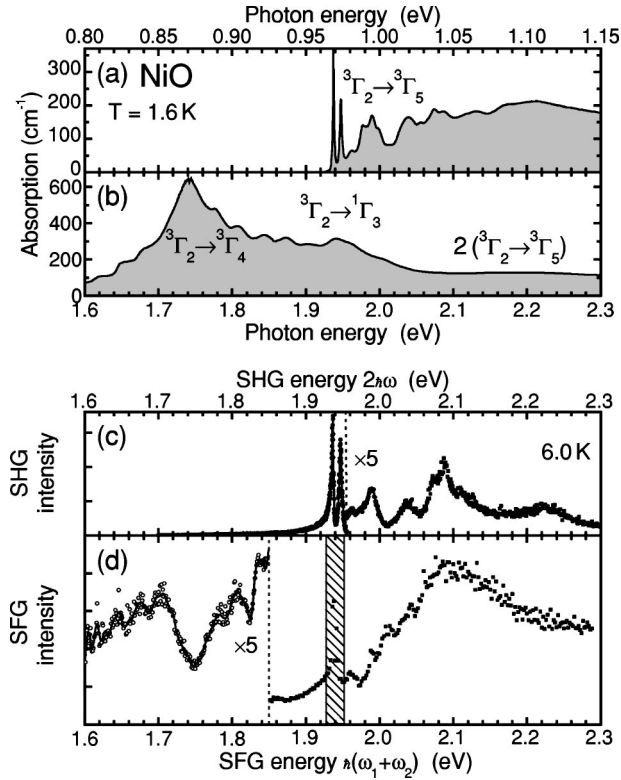


FIG. 1. (a) and (b) Linear absorption spectra, (c) SHG spectrum, and (d) SFG spectra of NiO. The solid line on top of the open circles in (d): derived by Fourier filtering.

$$\mathbf{P}(\omega_1 + \omega_2) \propto \hat{\chi}_{(21)}^{\text{eem}} \mathbf{E}(\omega_2) \mathbf{H}(\omega_1) + \hat{\chi}_{(12)}^{\text{eem}} \mathbf{E}(\omega_1) \mathbf{H}(\omega_2), \quad (1)$$

where \mathbf{E} and \mathbf{H} are the electric and magnetic fields, respectively. In agreement with the band symmetry of the octahedrally coordinated $\text{Ni}^{2+}(3d^8)$ ion the first single-photon transition, i.e., the transition leading from the ground state to the intermediate state is allowed as the MD process while the transitions from the intermediate state to the final state and back to the ground state can be described as the ED transitions with the contribution of a parity conserving phonon.⁴ Microscopically, the susceptibility $\hat{\chi}^{\text{eem}}$ is composed of

$$\hat{\chi}_{(21)}^{\text{eem}} \propto \sum_{g,n,n'} \frac{P_{gn} P_{nn'} M_{n'g}}{(\omega_1 + \omega_2 - \omega_{ng})(\omega_1 - \omega_{n'g})}, \quad (2)$$

$$\hat{\chi}_{(12)}^{\text{eem}} \propto \sum_{g,n,n'} \frac{P_{gn} P_{nn'} M_{n'g}}{(\omega_1 + \omega_2 - \omega_{ng})(\omega_2 - \omega_{n'g})}. \quad (3)$$

$\hbar\omega_{n'g}$ and $\hbar\omega_{ng}$ refer to the energy difference separating the ground-state $|g\rangle$ from the intermediate-state $|n'\rangle$ or the final-state $|n\rangle$, respectively. M and P are the matrix elements of the MD and ED operators, respectively. Note that $\hat{\chi}_{(21)}^{\text{eem}}$ and $\hat{\chi}_{(12)}^{\text{eem}}$ describe competing contributions to SFG. The intensity of the SFG signal is maximized by exciting one of them, e.g., $\hat{\chi}_{(21)}^{\text{eem}}$ resonantly at $\omega_{n'g} = \omega_1$ while $\hat{\chi}_{(12)}^{\text{eem}}$ is, in general, suppressed because of nonresonant excitation.

The experimental setup is detailed in Ref. 10. Figure 1 shows absorption, SHG, and SFG spectra of NiO. The SHG spectrum represents an inseparable convolution of electronic transitions at $\hbar\omega$ and $2\hbar\omega$ since with only one laser field

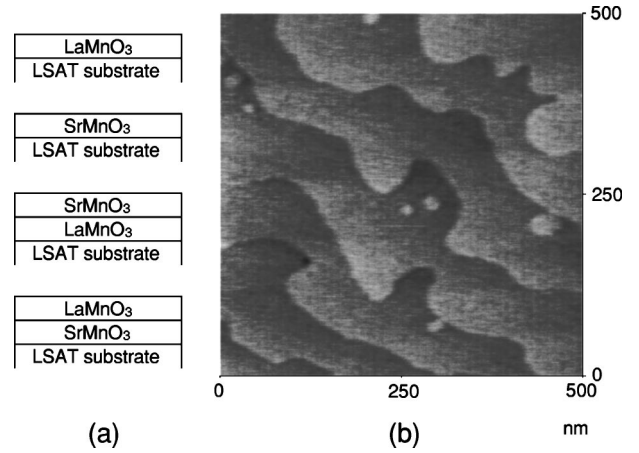


FIG. 2. (a) Schematic illustrations of manganite thin films on the LSAT substrates. (b) Atomic force microscope image of SrMnO_3 thin film. Steps with unit lattice height and terraces with about 100-nm width are clearly observable.

available, both the degree of resonance enhancement at $\hbar\omega$ and the two-photon spectrum at $2\hbar\omega$ are simultaneously tuned. The ${}^3\Gamma_2 \rightarrow {}^3\Gamma_4$ transition near 1.7–1.8 eV is not resolved because of the absence of intermediate resonant states at $\hbar\omega$. Figure 1(d) shows that these principal disadvantages are overcome by the SFG experiment. For SFG the photon energy $\hbar\omega_1$ of the intermediate state was fixed at 0.972 eV so that the transition ${}^3\Gamma_2 \rightarrow {}^3\Gamma_5$ is resonantly excited. Thus, the resonance provides the largest possible degree of enhancement for the whole SFG spectrum so that Fig. 1(d) shows the true nonlinear spectral dependence at $\hbar(\omega_1 + \omega_2)$. The ${}^3\Gamma_2 \rightarrow {}^3\Gamma_4$ transition is thus resolved and the phonon sidebands of the ${}^3\Gamma_2 \rightarrow {}^3\Gamma_4$ transition are reproduced. Further, a broad transition at around 2.1 eV which originates in the $2({}^3\Gamma_2 \rightarrow {}^3\Gamma_5)$ two-sublattice excitation is observed.¹⁰ The hatched region with the narrow peaks on top of the ${}^3\Gamma_2 \rightarrow {}^1\Gamma_3$ transition denotes the energy range where SFG at $\hbar(\omega_1 + \omega_2)$ from $\hat{\chi}_{(21)}^{\text{eem}}$ and $\hat{\chi}_{(12)}^{\text{eem}}$ and SHG at $2\hbar\omega_1$ and $2\hbar\omega_2$ are nearly degenerate and interfere with each other.

Intermediate levels for resonance enhancement can be found in all 3d compounds except those with an *S*-like ground state so that resonance-enhanced SFG constitutes a very general method for the investigation of centrosymmetric magnetic bulk compounds.^{5,11} The large intensities inherent to it are particularly useful in studies of the spin dynamics of antiferromagnetic systems where low signal amplitudes are a notorious problem.¹²

III. INTERFACE-SENSITIVE SHG

Manganite thin films (LaMnO_3 , SrMnO_3 , $\text{SrMnO}_3/\text{LaMnO}_3$, and $\text{LaMnO}_3/\text{SrMnO}_3$) were grown on $(\text{LaAlO}_3)_{0.3}-(\text{SrAl}_{0.5}\text{Ta}_{0.5}\text{O}_3)_{0.7}$ (LSAT) (001) substrates by pulsed laser deposition as illustrated in Fig. 2(a). During the deposition, the substrate temperature was kept at 760 °C for $\text{SrMnO}_3/\text{LaMnO}_3$ and $\text{LaMnO}_3/\text{SrMnO}_3$, 790 °C for SrMnO_3 , 800 °C for LaMnO_3 and the oxygen pressure at 0.1 mTorr. The LaMnO_3 and SrMnO_3 films were deposited in the two-dimensional layer-by-layer mode, which is confirmed by the oscillation of specular spot intensity in the

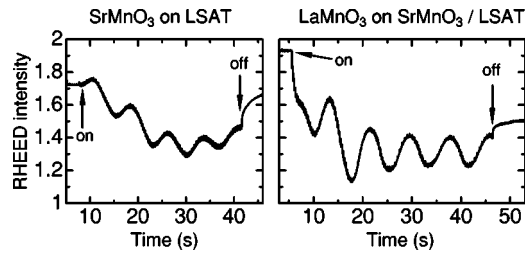


FIG. 3. The reflection high-energy electron diffraction (RHEED) intensity oscillations observed during the deposition of $\text{SrMnO}_3/\text{LaMnO}_3$ on LSAT (001) substrate.

reflection high-energy electron diffraction (RHEED). The thickness of each layer was regulated to be 4–5 unit cells by counting the number of RHEED oscillations as shown in Fig. 3. Figure 2(b) exemplifies an atomic force microscope (AFM) image of SrMnO_3 on LSAT. Terraces with about 100-nm width and the step height of one unit cell are clearly observable.

SHG was measured at room temperature in air by amplified 150-fs light pulses at a repetition rate of 1 kHz. The SH photon energy was fixed at 1.37 eV. The angle of the incident light with respect to the surface of the sample was varied from -90° to $+90^\circ$ in order to measure the Maker fringes¹³ for p -polarized incident and p -polarized transmitted SHG light. The fundamental light was incident from the back of the substrate in order to avoid the absorption of SH light in the LSAT substrate. Since the intensity and width of the incident light pulses fluctuate temporally, the signal was normalized by SHG on urea powder. The SHG signal was separated from the fundamental light by appropriate filters and a monochromator and detected by a photomultiplier tube. The signal was amplified by a low noise amplifier and collected by a boxcar integrator with averaging of typically 5000 pulses.

Figure 4 exemplifies the Maker fringe pattern of $\text{SrMnO}_3/\text{LaMnO}_3$ on LSAT. The other thin films show similar fringe shape. In general, SHG from thin films of centrosymmetric materials are described by the ED-allowed interface contribution and the nonlocal electric-quadrupole

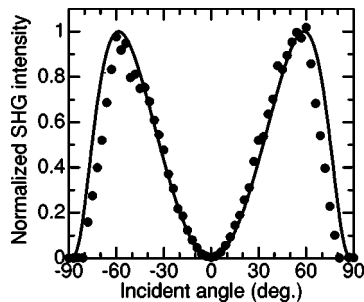


FIG. 4. Maker fringe of a manganite thin-film $\text{SrMnO}_3/\text{LaMnO}_3$ on LSAT. The angle of incidence is given with respect to the sample normal. A solid curve is a model calculation result.

(EQ) contribution.¹⁴ Negligible SHG signal from the substrate excludes the EQ contributions from the bulk and interface of the substrate. Since the SHG intensity is not dependent on the film thickness, EQ bulk contributions from the manganite films are also excluded. Consequently, the SHG signal originates in the ED contributions from the air- SrMnO_3 and SrMnO_3 - LaMnO_3 interfaces. Contribution from the LaMnO_3 -LSAT interface is negligible because the surface termination of the LSAT is not controllable.

A solid curve in Fig. 4 is a model calculation result assuming the existence of ultrathin nonlinear medium that possesses the tetragonal symmetry ($4mm$) at the interface. Good agreement with experimental data confirms that the SHG is emitted from the aforementioned interfaces and sensitive to the valence difference of Mn ions at the interface. Interface magnetism in perovskite manganites has also been investigated,^{15,16} but a spectroscopic study at the interface has not yet been reported. Magnetic SH spectroscopy will therefore be performed on these systems in a wide spectral range in the future.

IV. CONCLUSIONS

Two centrosymmetric magnetic systems were successfully investigated by the second-order nonlinear optics. Resonance-enhanced MD-type SFG has been introduced as a technique for studying the bulk properties of centrosymmetric magnetic materials of arbitrary symmetry. Interface-sensitive ED-type SHG was used to reveal the valence difference of Mn ions at the heterointerface of the manganite thin film. It will provide valuable contribution in the interface physics, in which local probes are clearly in need.

¹Y. R. Shen, *The Principles of Nonlinear Optics* (Wiley, New York, 1984).

²*Nonlinear Optics in Metals*, edited by K. H. Bennemann (Clarendon, Oxford, 1998).

³M. Fiebig, V. V. Pavlov, and R. V. Pisarev, a special issue on J. Opt. Soc. Am. B **22**, 96 (2005).

⁴M. Fiebig, D. Fröhlich, Th. Lottermoser, V. V. Pavlov, R. V. Pisarev, and H. J. Weber, Phys. Rev. Lett. **87**, 137202 (2001).

⁵M. Fiebig, Th. Lottermoser, V. V. Pavlov, and R. V. Pisarev, J. Appl. Phys. **93**, 6900 (2003).

⁶M. Fiebig, K. Miyano, Y. Tomioka, H. Kuwahara, Y. Tokura, and K. Reimann, Phys. Rev. Lett. **86**, 6002 (2001).

⁷M. Izumi *et al.*, Phys. Rev. B **64**, 064429 (2001).

⁸K. S. Takahashi, M. Kawasaki, and Y. Tokura, Appl. Phys. Lett. **79**, 1324 (2001).

⁹Y. Ogimoto, M. Izumi, A. Sawa, T. Manako, H. Sato, H. Akoh, M. Kawasaki, and Y. Tokura, Jpn. J. Appl. Phys., Part 2 **42**, L369 (2003).

¹⁰T. Satoh, Th. Lottermoser, and M. Fiebig, Appl. Phys. B: Lasers Opt. **79**, 701 (2004).

¹¹Y. Tanabe and S. Sugano, J. Phys. Soc. Jpn. **9**, 753 (1954).

¹²N. P. Duong, T. Satoh, and M. Fiebig, Phys. Rev. Lett. **93**, 117402 (2004).

¹³P. D. Maker, R. W. Terhune, M. Nisenoff, and C. M. Savage, Phys. Rev. Lett. **8**, 21 (1962).

¹⁴P. S. Pershan, Phys. Rev. **130**, 919 (1963).

¹⁵Y. Ogawa, H. Yamada, T. Ogasawara, T. Arima, H. Okamoto, M. Kawasaki, and Y. Tokura, Phys. Rev. Lett. **90**, 217403 (2003).

¹⁶H. Yamada, Y. Ogawa, Y. Ishii, H. Sato, M. Kawasaki, H. Akoh, and Y. Tokura, Science **305**, 646 (2004).